Int. J. Heat Mass Transfer. Vol. 35, No. 8, pp. 2005–2016, 1992
Printed in Great Britain

0017–9310/92 $5.00 + 0.00

Forced convection film boiling in the stagnation region of a molten drop and its application to vapour explosions

T. R. FODEMSKI

NNC Ltd, PWR Systems Dept., Booths Hall, Chelford Road, Knutsford, Cheshire WA16 8QZ, U.K.

(*Received* 24 *June* 1991 *and in final form* 15 *July* 1991)

Abstract—This work was undertaken as part of an investigation into the heat transfer mechanism related to thermal explosion. The theoretical model of forced convection film boiling in the stagnation point region of an axi-symmetrical molten drop is presented. The model is particularly relevant to the coarse pre-mixing stage of vapour explosion: it takes account of the fact that, at this stage, the hot substance is molten. Stagnation point momentum (Falkner–Skan) and energy equations, for cold and hot liquids and for the vapour layer, were solved numerically, with a wide range of boundary-matching conditions at the interfaces. The model presented, by covering a wide range of the conditions and parameters, is more general than the cases discussed in other publications. For this reason the results can be applied not only to the coarse pre-mixing stage of vapour explosion, but also to other situations, where three-phase forced convection occurs on an axi-symmetrical body.

1. INTRODUCTION

THE ANALYSIS of vapour explosion has been a subject of interest over many years. This phenomenon sometimes occurs when hot (molten) material mixes with more volatile liquid. To be precise vapour explosion can be considered as a subset of different outcomes of such a mixing. It is, however, most dangerous, resulting in massive rapid vapour generation, accompanied by destructive pressure wave and mechanical work upon the surroundings. The possibility that this phenomenon might occur in liquid-cooled nuclear reactors, as a result of serious reactor core overheating [1, 2], emphasizes its importance and has been the reason for extensive investigations (although it is fair to say that the earliest work was initiated by the metallurgical industry; this type of explosion has also been recorded in liquefied natural gas and paper industries and is known to occur when molten lava from volcanic eruptions encounters water).

In the case of liquid-cooled nuclear reactors, under some circumstances, the integrities of reactor vessel and/or containment could be challenged [2, 3] with the possible release of substantial quantities of fission products to the environment. Although such possibilities are considered remote the consequences could be so serious that a thorough understanding and realistic modelling of crucial stages of the phenomenon are required.

The conditions which determine whether an efficient, energetic and large-scale vapour explosion will occur are still rather uncertain [1–4]. However, there is a general consensus that one of the preconditions for a large-scale vapour explosion is the occurrence of a so-called coarse pre-mixing stage. During this stage hot liquid in the form of particles of size 1–2 cm is mixed with the pool of liquid coolant. There is relative movement between the components, but they are prevented from intimate contact by a vapour blanket of the coolant. If this vapour film is stable a substantial volume of this coarse mixture might be produced. Knowledge of the events in this mixing stage, leading to vapour collapse, is particularly important. Various models of film boiling heat transfer from a (hemi-)sphere have been published [5–8]. They are applicable to the case of a hot particle in the solid state and therefore have limited relevance to the coarse pre-mixing stage.

The model presented here takes account of the fact that, at this stage, the hot substance is molten. It considers the forced convection film boiling in the stagnation point region of an axi-symmetrical molten drop. On the basis of this model an accurate value of the vapour layer thickness in this region can be calculated, together with heat fluxes in the cold and hot liquids. This thickness at the stagnation point is of paramount significance, since it is minimal there, and it also determines the thickness of the vapour layer around the whole particle. As shown in refs. [9–11] it also constitutes a main parameter affecting stability and vapour film collapse (self-triggered or induced by a pressure pulse).

2. PHYSICAL MODEL

The analysis in this study is limited to the stagnation point region. The main aims of the work are:

NOMENCLATURE

a	constant
A	stagnation point velocity gradient
b	constant
c_p	specific heat at constant pressure
d	coefficient, ratio of heat fluxes
$e(\eta)$	function defined by equation (12)
$E(\eta)$	function defined by equation (13)
f	function
$F(\eta)$	dimensionless fluid flow stream function (its value at interface I, $F(0)$, describes evaporation)
g	gravitational acceleration
h	latent heat
k	thermal conduction
m	evaporation mass rate
N	coefficient in equation (1)
p	pressure
Pr	Prandtl number
q	heat flux
R	radius of molten fuel drop
$t(\eta)$	dimensionless fluid temperature, defined by equation (8)
T	temperature
ΔT	temperature difference
u	velocity
x, y	coordinates.

Greek symbols

α	coefficient, ratio of material parameters on interface II
β	coefficient, ratio of material parameters on interface I
δ	vapour thickness
ε	emissivity
η	dimensionless similarity coordinate in fluid
θ	angle (in x direction)
κ	thermal diffusivity
λ	dimensionless vapour thickness
μ	dynamic viscosity
ν	kinematic viscosity
ξ	dummy variable
ρ	density
σ	radiant constant.

Subscripts or superscripts

ev	evaporation
f	value for molten fuel
l	value for liquid coolant
pot	value for a frictionless flow
r	radiation
s	saturation value
v	value for vapour coolant
w	hot surface value
x	around the particle component
y	normal to the particle (interface) component
∞	value at infinity (free stream) or far from the interface
δ	value at interface I
*	normalized, dimensionless value
0	reference value or non-shear stress value.

- detailed analysis of the flow of liquid around the axi-symmetrical particle, in the vicinity of the liquid–vapour interfaces, when a significant distortion from the frictionless flow case takes place;
- analysis of the influence of this distortion on the heat transfer, particularly on the heat flux at the liquid interface;
- detailed analysis of the flow and heat transfer in the vapour layer—both determined by flows in the hot and in the cold liquids and also by heat transfer between them; and
- theoretical analysis leading to an approximate formula for a 'terminal' velocity of molten particles (surrounded by vapour) free-falling in the liquid.

The following assumptions have been made:

1. The liquid flow away from the interface approaches the frictionless case (both in the cold and hot liquids; see Fig. 1).

2. The vapour layer is thin compared with the particle size.

3. The vapour velocity has two components (in the x and y directions). The vapour velocity towards the hot surface (this component is not shown in Fig. 1) varies from maximum at the coolant interface to zero at the hot surface. The flow in the vapour around the molten particle occurs as a result of the pressure gradient produced by the movement, with constant velocity, u_∞, of this particle through coolant, and also because of the motions of the cold and the hot liquids at their respective interfaces with the vapour (see I and II in Fig. 1).

4. The coolant interface temperature is constant (at the saturation value T_s), while its free stream temperature is $T_{l\infty}$.

5. The temperature at the hot particle interface, T_w, is constant and away from this surface (but still in the region of the stagnation point) it is $T_{f\infty}$.

6. The vapour layer is transparent to the radiation heat flux. All the radiation heat flux is absorbed at the liquid–vapour interface (see I in Fig. 1).

7. All physical properties of the two liquids are assumed to be constant and taken for their average temperature.

8. The vapour properties are assumed to be different at the three locations:

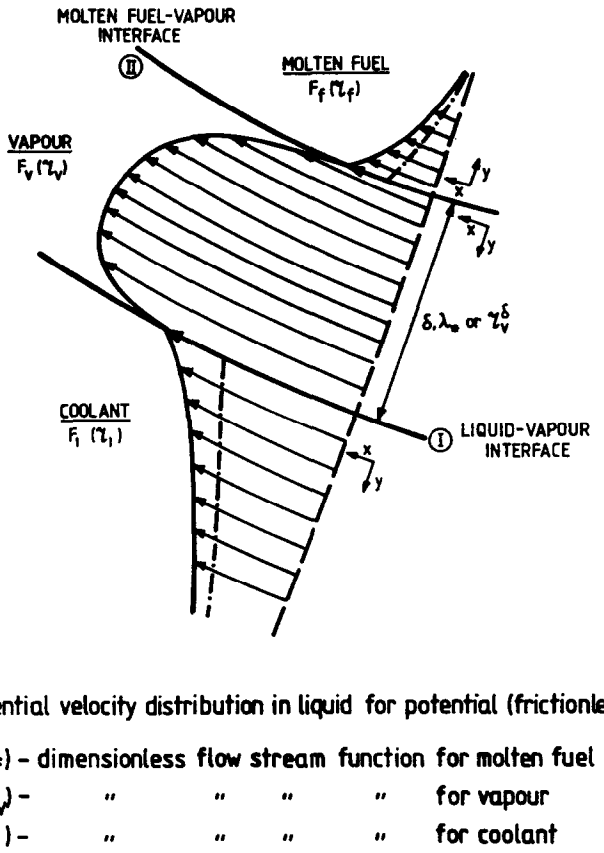

—·—·— Tangential velocity distribution in liquid for potential (frictionless) flow

$F_f(\eta_f)$ - dimensionless flow stream function for molten fuel

$F_v(\eta_v)$ - " " " " for vapour

$F_l(\eta_l)$ - " " " " for coolant

FIG. 1. Three-phase stagnation point arrangement.

(i) interface I, taken for the liquid coolant saturation temperature, T_s;
(ii) interface II, taken for the hot particle surface temperature, T_w; and
(iii) vapour gap, taken for the average temperature across this gap.

The last assumption attempts to represent the significant variation of the vapour properties over the wide temperature range (up to 2900 K). It follows the assumption made in ref. [12].

2.1. *Momentum equation and velocity field for the liquids*

The momentum equation for a fluid in the region of the stagnation point, considered in this study, has the form:

$$F''' + NF''F - F'^2 + 1 = 0. \tag{1}$$

It is worth noting that the above equation is the special form of the Falkner–Skan equation for similar flow, giving a solution for boundary layer thickness independent of x (see Fig. 1). Since the solution of equation (1) and all boundary conditions (see further discussion) are also independent of x, although there is transport of mass and enthalpy in the x direction, there are no temperature gradients in this direction, in the vapour or either of the liquids, in the region of validity of the equations.

For an axi-symmetrical body, considered in this study, $N = 2$ (for a two-dimensional case $N = 1$). The dimensionless flow stream function F depends on the dimensionless similarity coordinate η, given by

$$\eta = \sqrt{\left(\frac{2A}{\nu}\right)} y \tag{2}$$

(this form of the momentum equation is different from that used in ref. [7], but equation (1) can be obtained by assuming $\phi(\xi) = \sqrt{2F(\eta)}$ and $\xi = \sqrt{2\eta}$ in ref. [7]). Velocity components in the x and y directions are given by

$$u_x = Ax\frac{dF}{d\eta}; \quad u_y = -\sqrt{(2A\nu)}F(\eta) \tag{3}$$

and A is the velocity gradient at the stagnation point.

The inclusion of the possibility of significant departure of the liquid flow from the frictionless solution, for a thin layer close to the interface, means that an analytical solution (as in ref. [7], where only slight perturbation close to the interface was assumed) cannot be found and only a numerical one can be achieved. It is worth mentioning that previously,

equation (1) has been solved numerically (see, for example, ref. [13]) for the case of the stagnation point flow at a rigid, impermeable wall, i.e. with the following boundary conditions:

$$F(0) = 0; \quad F'(0) = 0 \quad \text{and} \quad \lim F'(\infty) = 1. \quad (4)$$

As was pointed out in ref. [7], the case of a fluid–fluid interface is different from that of a fluid–rigid wall. Firstly, the value of $F(0) \neq 0$ (if, for example, intense evaporation were to take place) and, secondly, the value of $F'(0)$ is not zero. Because equation (1) is of third order, it is obvious that for an assumed value of $F(0)$ there is one value of $F''(0)$ corresponding to each given value of $F'(0)$ which satisfies the condition $\lim F'(\infty) = 1$. Therefore the following can be written:

$$F''(0) = f[F(0), F'(0)]. \quad (5)$$

The above relation has been established by numerical integration of equation (1). It covers a wide range of values of $F(0)$ and $F'(0)$, i.e. from 0 to 1 and from 0 to 5, respectively. These ranges include cases considered in refs. [7, 13]. Agreement between values quoted in these other studies with the results presented here, in the 'overlapping' ranges of F and F', is excellent. For example, boundary conditions (4) were found to be satisfied for $F'' = 1.3119$ against 1.312 quoted in ref. [13]. It was also found that the following algebraic formula:

$$F'' = (a_1 + a_2 F + a_3 F^2)(1 - F') \times \sqrt{(1 + b_1 F'(1 + b_2 F + b_3 F^2))} \quad (6)$$

where

$$a_1 = 1.312 \quad a_2 = 1.2363 \quad a_3 = 0.21167$$

$$b_1 = 0.812 \quad b_2 = -1.1374 \quad b_3 = 0.46034$$

approximates all results obtained within 1.4%. This formula is useful in numerical calculations connected with any stagnation point flow.

2.2. *Energy equation and temperature field for the liquids*

The energy equation for a liquid in the region of the stagnation point has the general form

$$t'' + N\,Pr\,F(\eta)t' = 0 \quad (7)$$

where

$$t(\eta) = \frac{T(\eta) - T_{int}}{T_s - T_{int}} \quad (8)$$

and T_{int} is the interface temperature, and equation (8) defines dimensionless fluid temperature.

The boundary conditions for equation (7) are

$$t(0) = 0 \quad \text{and} \quad t(\infty) = 1. \quad (9)$$

The general solution of (7) has the form

$$t'(\eta) = \frac{e(\eta)}{E(\infty)} \quad (10)$$

and

$$t(\eta) = \frac{E(\eta)}{E(\infty)} \quad (11)$$

where

$$e(\eta) = \exp\left[-2Pr \int_0^\eta F(\xi)\,\mathrm{d}(\xi)\right] \quad (12)$$

and

$$E(\eta) = \int_0^\eta e(\xi)\,\mathrm{d}(\xi). \quad (13)$$

When Pr, the Prandtl number, is known, the dimensionless temperature gradient expressed by equation (10) can be calculated analytically only for the frictionless case without evaporation from the interface (i.e. $F(\eta) = \eta$ and $F(0) = 0$). For this case, the interface heat flux is expressed by [7, 14]

$$q_{pot} = 2k\sqrt{\left(\frac{Pr\,A}{\pi v}\right)}\Delta T. \quad (14)$$

The temperature difference ΔT for the liquid coolant is $(T_s - T_{l\infty}) = \Delta T_l$ and for the molten drop is $(T_{f\infty} - T_w) = \Delta T_f$.

For other, more general cases and for different Prandtl numbers, this interface heat flux has been calculated numerically and the results are presented in Figs. 2 and 3. Figure 2 shows the ratio, d_1, of two heat fluxes: (i) when $F'(0) = 1$, but $F(0)$ is in the range of 0 to 1, and (ii) for the frictionless, without evaporation case, i.e. the one expressed by equation (14). This ratio shows the effect of the evaporation from the interface on the heat flux there, when there is no velocity distortion caused by viscous forces. Figure 3((a)–(f), for different Pr) shows the ratio, d_2, of the interface heat fluxes: (i) for any value of F and F' in the ranges 0 to 1 and 0 to 5, respectively, and (ii) for the same value

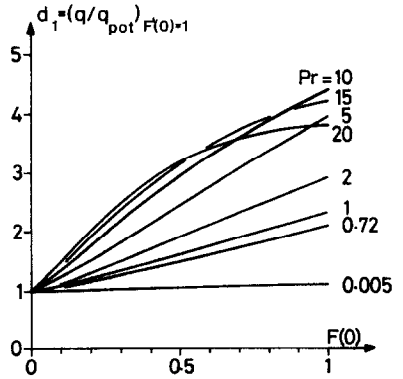

FIG. 2. Effect of the interface evaporation, $F(0)$, on the normalized liquid interface heat flux, for different Pr numbers. Note that all values are for $F'(0) = 1$.

of F as before, but with $F' = 1$. The combined effect of

- the viscous forces (which affect the velocity distribution in the vicinity of the interface), and
- the evaporation from the interface (which increases the velocity component towards this interface)

on the interface heat flux in the liquid, in comparison to that given by (14), is therefore expressed by the product $d_1 d_2$.

2.3. *Velocity field for the vapour layer*

The same momentum equation (1) describes the vapour flow in the stagnation point region of the vapour layer, but boundary conditions are more complicated than before. According to assumption 3 the coolant flow 'drives' not only the vapour flow but also, through the vapour, the flow in the molten drop. It was assumed that the pressure gradients in all fluids in the stagnation point region are the same; therefore the following can be written:

$$\rho_l A_l^2 = \rho_v A_v^2 = \rho_f A_f^2. \tag{15}$$

Strictly speaking this assumption is valid for fluid jets meeting to form a plane interface at the stagnation point (such geometry was considered, for example, in ref. [13]). However, the same equation (15) is used for the present model as it has been used for other cases with fluids forming an axi-symmetrical/spherical interface (see, for example, refs. [6, 7, 13–15]). This is an approximation, since for a convex interface the pressure in the inside medium is increased by the surface tension contribution. There are two reasons why this simplification is still in the present analysis:

1. The exact radius of curvature (of a molten drop,

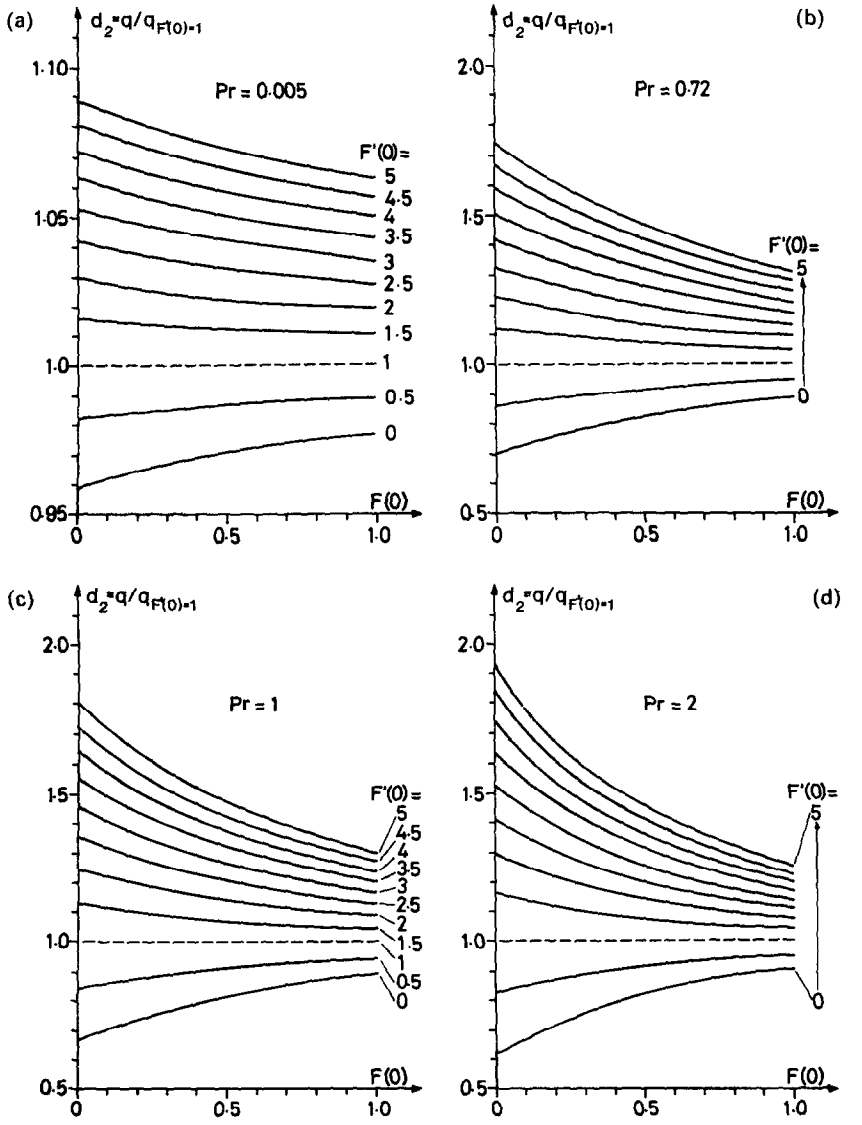

FIG. 3. Effect of the interface evaporation, $F(0)$, and the interface tangential velocity, $F'(0)$, on the normalized liquid interface heat flux, for different Pr.

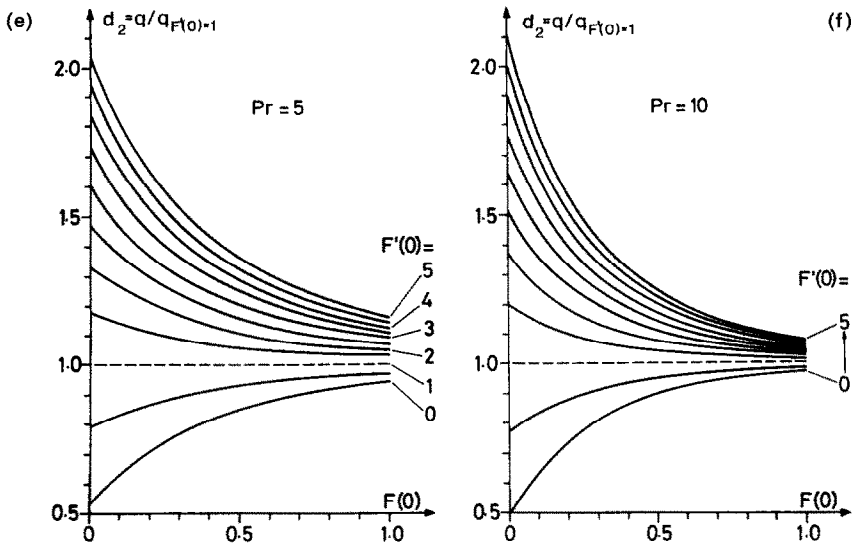

FIG. 3.—*Continued.*

at the stagnation point) can only be found by a complete solution of the flow field inside the drop and its interaction with the entire outside fluids. This is, however, outside the scope of this work.

2. The reliable value of surface tension for molten UO_2 is hardly known. (It is also important to remember that the variation of this surface tension, with the temperature close to the freezing point, can result in additional tangential force on the interface. Also, this effect, apart from lack of data, is again outside the scope of the presented work.)

For the molten drop case considered in this study, the full equation (1) was solved numerically, with equation (15) and the following boundary-matching conditions on the interfaces I and II, respectively

$$F_v(\eta_v^\delta) = \beta_2 F_l(0) \quad F_v'(\eta_v^\delta) = \beta_1 F_l'(0)$$
$$F_v''(\eta_v^\delta) = \beta_1\beta_2 F_l''(0) \tag{16}$$

$$F_v(0) = 0 \quad F_v'(0) = \alpha_1 F_f'(0) \quad F_v''(0) = -\alpha_2 F_f''(0) \tag{17}$$

$$\beta_1 = 1/\sqrt{(\rho_l^*)} \quad \beta_2 = \sqrt{(\mu_l^*/\beta_1)}$$
$$\rho_l^* = \rho_l/\rho_v \quad \mu_l^* = \mu_l/\mu_v \tag{18}$$

$$\alpha_1 = 1/\sqrt{(\rho_f^*)} \quad \alpha_2 = \sqrt{(\mu_f^*\alpha_1)}$$
$$\rho_f^* = \rho_f/\rho_v \quad \mu_f^* = \mu_f/\mu_v. \tag{19}$$

Relations (16) and (17) express equality of mass fluxes and of appropriate velocity and shear stress components on both sides of each interface. Note that the evaporation flux is present on interface I, but interface II was assumed to be impermeable.

The results of the momentum equation integration for the vapour layer cannot be presented in general and compact form. There are two reasons for this. Firstly, material parameters of all fluids have to be specified, i.e. the values of coefficients α_1, α_2, β_1 and β_2 (they vary considerably for any fluid pair and also with temperature and pressure). Secondly, the vapour velocity profile strongly depends upon the vapour thickness. Since this thickness results from the heat balances on both interfaces, this practically means that momentum (1) and energy (6) equations have to be solved simultaneously. As in ref. [7], the vapour thickness δ is related to the vapour similarity coordinate, η_v, and normalized vapour thickness, λ_*, both dimensionless, in the following way:

$$\eta_v(\delta) = \eta_v^\delta = \delta\sqrt{(2A_v/v_v)} \quad \eta_v^\delta = 2\lambda_*/(\rho_l^*)^{1/4} \tag{20}$$

$$\lambda = \delta\sqrt{(A_l/(2\kappa_v))} \quad \lambda_0 = \sqrt{(Pr_v/\rho_l^*)}$$
$$\lambda_* = \lambda/\lambda_0 = \delta\sqrt{(A_l\rho_l/(2\mu_v))}. \tag{21}$$

Values λ_0 and $\lambda_* = 1$ have clear physical interpretation. Both are functions of material parameters only (!), and refer to the vapour thickness for which velocity distribution, in the vapour gap, is perpendicular to the liquid–vapour interface. For such distributions there is no shear on this interface and, consequently, the velocity field in the liquid is as for a frictionless case [7]. For $\lambda_* > 1$, liquid is accelerated by vapour flow, but for $\lambda_* < 1$ the situation is reversed ($\lambda_* = 0$ is the extreme case of a solid wall). In ref. [7] the range of λ_* was limited to about 3 (and the hot surface was rigid), but the present model, for the coarse pre-mixing stage of vapour explosion, does not have any limitation.

2.4. *Temperature field in the vapour layer*

The solution, (10) and (11), of the energy equation (7), for the vapour, depends upon the dimensionless temperature and boundary conditions given by

$$t_v(\eta_v) = \frac{T(\eta_v) - T_w}{T_s - T_w} \tag{22}$$

$$t_v(0) = 0 \quad \text{and} \quad t_v(\eta_v^\delta) = 1 \tag{23}$$

where T_w is the temperature of the hot interface and T_s is the temperature of the vapour–liquid interface (saturation temperature).

As in the liquid, respective integrals can only be calculated numerically. The ratio, d_3, of the heat fluxes on interfaces II, q_w, and I, q_δ, is not equal to 1 since, in this case, the vapour velocity towards the hot surface is taken into account. Also the ratio, d_4, of the interface I heat flux, q_δ, and the heat flux calculated for simple conduction through stagnant vapour of the same thickness is, in general, also not equal to 1. The latter is expressed by the relation:

$$q_0 = k_v(T_w - T_s)/\delta. \tag{24}$$

The ratios d_3 and d_4 depend not only upon the vapour layer thickness, δ, but also, through α_1, α_2, β_1 and β_2, upon material properties.

The heat balances on the interfaces I and II can be written in the following form:

$$\text{I}: q_l + q_{cv} = q_r + q_\delta; \quad \text{II}: q_f = q_w + q_r \tag{25}$$

where

$$q_l = d_{l1}d_{l2}q_{lpot}; \quad q_{ev} = m_v h;$$
$$m_v = \rho_v u_{yv}(\delta) = \rho_v\sqrt{(2A_v v_v)}F_v(\eta_v^\delta)$$
$$q_r = \sigma(T_w^4 - T_s^4)/(1/\varepsilon_l + 1/\varepsilon_f - 1); \quad q_\delta = d_4 q_0$$
$$q_f = d_{f2}q_{fpot}; \quad q_w = d_3 q_\delta = d_3 d_4 q_0.$$

Ratios d_3 and d_4 must be calculated numerically. However, when inertia effects can be neglected (this is the case at atmospheric pressure for both UO_2–H_2O and UO_2–liquid Na considered later in the paper), solution of the problem is simplified. This case, discussed in the Appendix, can also serve as an example of the calculation route for the whole problem, i.e. simultaneous solution of the momentum and energy equations for three fluid phases.

3. TERMINAL VELOCITY OF THE FREE-FALLING MOLTEN DROP

When a molten drop of high temperature falls through a stagnant pool of more volatile liquid, the intensive evaporation of the latter takes place. There is experimental evidence (examples being refs. [16, 17]) that the wake behind this drop has an almost cylindrical shape, as shown in Fig. 4. The full analysis of all processes in this wake is a formidable task. However, from the wake shape it is obvious that the vapour pressure in the equatorial cross-section of the drop is very much the same as in the whole wake. Assuming that the bottom part of the drop is spherical and that the velocity and pressure gradient on the liquid–vapour interface (curve between points A and S in Fig. 4) follow the appropriate frictionless case distributions, one can use the well-known relations

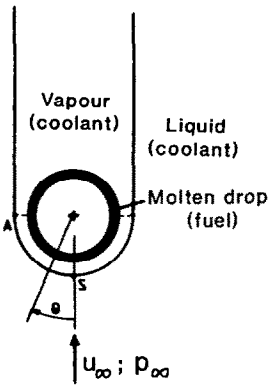

FIG. 4. Free-falling molten drop in liquid arrangement.

$$p_\theta + \frac{\rho_l u_\theta^2}{2} = \text{const}; \quad u_\theta = \tfrac{3}{2}u_\infty \sin\theta \tag{26}$$

and

$$p_\theta - p_A = \tfrac{9}{8}\rho_l u_\infty^2 \cos^2\theta. \tag{27}$$

For a free-falling drop: (i) gravitational force and (ii) the force exerted on the spherical drop from the fluid are equal, i.e.

$$\tfrac{4}{3}\pi R^3 \rho_f g = \int_0^{\pi/2} 2\pi R \sin\theta (p_\theta - p_A) R\cos\theta \, d\theta. \tag{28}$$

Substituting (27) into (28)

$$u_\infty = \sqrt{((64/27)Rg\rho_f/\rho_l)}. \tag{29}$$

The last formula is approximate. However, it compares well with the experimental results, quoted in refs. [16, 17] (where molten drops of different substances were allowed to fall in pools of different coolants). Based on this terminal velocity, its gradient at the liquid coolant stagnation point, A_l, can be expressed by

$$A_l = \frac{3}{2}\frac{u_\infty}{R} = 4\sqrt{\left(\frac{g\rho_f}{3R\rho_l}\right)}. \tag{30}$$

4. EXAMPLES AND CONCLUSIONS

4.1. *Example of molten* UO_2 *drops falling in water or in liquid sodium*

This section presents numerical results of the model discussed in this study, applied to cases of a molten UO_2 drop of 1 cm diameter, free-falling in water (which is at pressures of 1 and 150 bar) and in liquid sodium (1 bar). The two different pressures for water correspond to ex- and in-vessel conditions of PWR (the lower pressure for water also corresponds to BWR conditions).

The material properties of molten UO_2 are difficult to find in the open literature. It is worth noting that all these properties are affected by fuel burn-up and accumulation of plutonium and fission products.

This refers particularly to the temperature difference between the boiling and melting points of UO_2, i.e. the maximum temperature difference which can exist in the molten drop. Information in the literature (ref. [17] and also ref. [18]) indicates that this difference could be somewhere in the range 500–1400 K. The following material values were used in all the calculations presented here [17, 18]:

$$\rho_f = 8500\,\mathrm{kg\,m^{-3}}, \quad Pr_f = 1,$$

$$c_{pf} = 0.5\,\mathrm{kJ\,kg^{-1}\,K^{-1}}, \quad k_f = 2\,\mathrm{W\,m^{-1}\,K^{-1}},$$

$$\varepsilon_f = 0.8$$

and a melting point temperature for UO_2 of 3000 K (the molten drop interface II, see Fig. 1, was assumed to be always at this temperature). All coefficients appearing in Section 2.3 (α_1, α_2, β_1 and β_2), approximate terminal drop velocity and its gradient at the liquid coolant stagnation point (u_∞ and A_1, calculated from equations (29) and (30), respectively), dimensionless vapour thickness, λ_0, emissivity of the liquid–vapour interface, ε_i, and radiative heat flux q_r for all three cases considered, are presented in Table 1. Water, steam, liquid and vapour sodium properties, under high temperatures and appropriate pressure (see assumptions 7 and 8) were approximated from refs. [19–22]. The maximum liquid coolant and molten drop subcoolings (determined by the appropriate temperature difference between boiling and melting points) are also presented in Table 1 (rows 8 and 9).

It is worth adding that any uncertainty connected with values of material parameters and also with simplifications (for example, equation (15)) and their importance in the model can be estimated by so-called sensitivity studies in which the presented examples could be regarded as base cases.

The results of the calculations are presented in Table 1 and in Figs. 5–9.

Rows 10 and 11 of Table 1 give the range of the dimensionless normalized vapour thickness, λ_*, and $(\delta/R)_{max}$ (for the highest value of λ_*), respectively, for all three cases considered. Since the relation between λ_* and δ is linear (see equation (21)), the latter can be determined for any value of the former. However, realistic conditions of pre-mixing are such that the corresponding values of λ_* are always away from their respective bottom limits. The minimum value of λ_* for water represents the case when the bulk liquid coolant temperature is equal to the freezing temperature. Quoted values of $(\delta/R)_{max}$, for maximum λ_*, correspond to the case when $T_{l\infty} = T_s$ (see also Fig. 9). These values also show that assumption 2 is satisfied in all three cases.

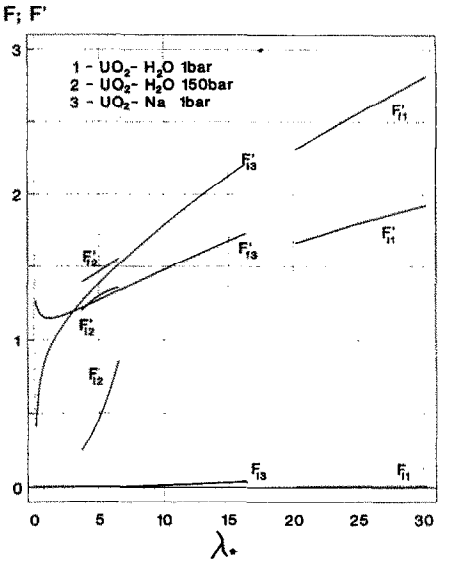

FIG. 5. Influence of the dimensionless, normalized vapour thickness, λ_*, on the stream function and its derivative values, $F(0)$ and $F'(0)$, in liquid coolant and molten fuel.

Figure 5 shows the influence of the dimensionless vapour thickness λ_* on values of the interface stream function, $F(0)$, and its first derivative, $F'(0)$, in the hot and cold liquids, for all three cases. It is worth noting that for UO_2–H_2O (150 bar) case values of $F(0)$ cover

Table 1

Quantity	Case: UO_2–H_2O 1 bar	UO_2–H_2O 150 bar	UO_2–Na 1 bar
1. α_1	2.70×10^{-3}	4.061×10^{-2}	3.293×10^{-3}
2. α_2	3.65×10^{-1}	1.370	0.6456
3. β_1	2.497×10^{-2}	3.994×10^{-1}	1.897×10^{-2}
4. β_2	30.49	2.688	17.842
5. u_∞ [m s^{-1}]	1.015	1.279	1.154
A_1 [s^{-1}]	3.05×10^{2}	3.84×10^{2}	3.46×10^{2}
6. λ_0	9.976×10^{-3}	1.462×10^{-1}	1.611×10^{-2}
7. ε_i	0.95	0.95	0.15
q_r [MW m^{-2}]	3.581	3.575	0.660
8. ΔT_{lmax} [K]	100	342	780
9. ΔT_{fmax} [K]	500–1400	500–1400	500–1400
10. λ_*	20.2–30.2	3.7–6.5	1–16.3
11. $(\delta/R)_{max}$	5.21×10^{-2}	1.27×10^{-2}	2.44×10^{-2}

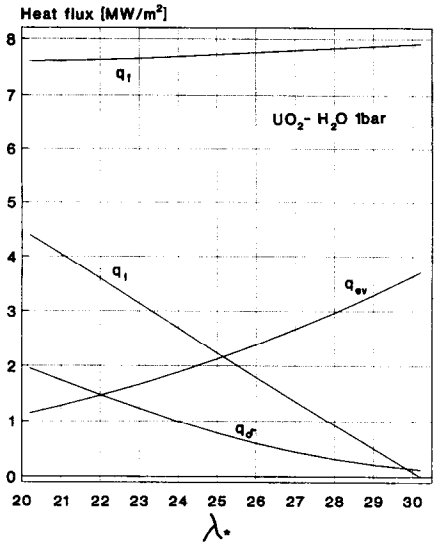

FIG. 6. Changes of heat fluxes at the interfaces I (q_{ev}, q_δ and q_l) and II (q_f) with the dimensionless normalized vapour thickness, λ_*.

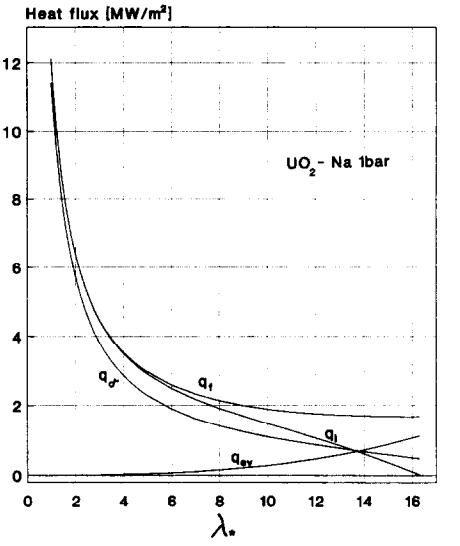

FIG. 8. Changes of heat fluxes at the interfaces I (q_{ev}, q_δ and q_l) and II (q_f) with the dimensionless normalized vapour thickness, λ_*.

the range from 0 to 1. Values of $F''(0)$ in each case, for both the hot and the cold liquids, can be calculated from equation (6).

Figures 6–8 show the heat at the interfaces I (q_l, q_δ and q_{ev}) and II (q_f) as functions of the dimensionless vapour thickness λ_*, in the appropriate range for each case.

For UO_2–H_2O cases the heat flux at the molten drop interface, q_f, remains almost constant, i.e. almost independent of liquid subcooling and, therefore, of the liquid coolant interface temperature gradient. This independence justifies assumption 6, although it is shown in ref. [12] that for water the absorption of the q_r-flux (of the order as shown in Table 1) requires about 0.5 mm (for sodium all q_r is absorbed at the interface). For UO_2–H_2O at 1 atm (Fig. 6) the heat flux associated with conduction through the vapour gap, q_δ, is smaller than the radiative flux, q_r (see Table 1, row 7). For the UO_2–H_2O (150 atm) case, the heat flux q_δ is greater than q_r for almost the whole range of λ_*.

The case of UO_2–Na presented in Fig. 8 (and in Fig. 9 with others) differs from UO_2–H_2O cases. The high value of the liquid sodium thermal conductivity is responsible for that. For the range of λ_* between 9

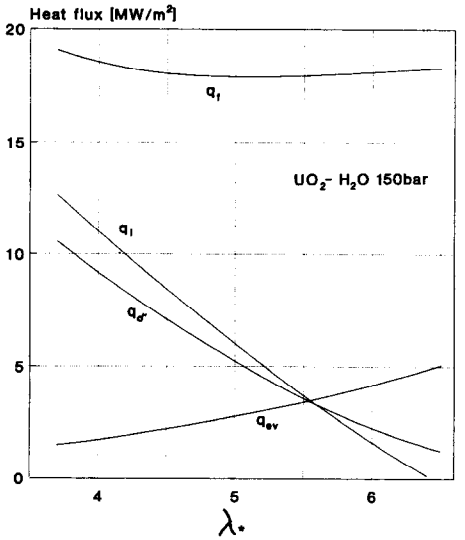

FIG. 7. Changes of heat fluxes at the interfaces I (q_{ev}, q_δ and q_l) and II (q_f) with the dimensionless normalized vapour thickness, λ_*.

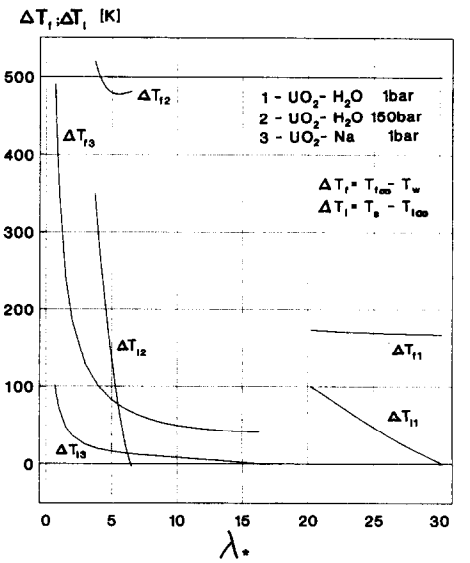

FIG. 9. Influence of the dimensionless, normalized vapour thickness, λ_*, on the temperature differences in molten fuel (ΔT_f), and in liquid coolant (ΔT_l). Note that in all cases $T_w = 3000$ K.

and 16, related to very small subcoolings ($\Delta T_{13} < 20$ K, see Fig. 9), the pattern of heat fluxes is similar to those in Figs. 6 and 7, with both $q_f \approx 2$ MW m^{-2} (see Fig. 8) and $\Delta T_f < 70$ K (see ΔT_{f3} in Fig. 9) being even smaller than for water cases. The situation changes drastically when the lower limit of λ_* is approached. This lower limit is adopted to be equal to 1 (although it occurs for subcooling of only about 100 K from 780 K available). There are two facts, however, supporting this limit. Firstly, it coincides with the calculated temperature difference ΔT_f, in the drop, of about 500 K (the lower limit of ΔT_{fmax}). Secondly, there is no experimental evidence that forced convection film boilings on axi-symmetrical bodies are stable when the vapour dimensionless normalized thickness, λ_*, approaches the value 1. (It is still worth adding that the presented model predicts only for the UO_2–Na case that the upper limit of $\Delta T_{fmax} = 1400$ K has to be present in the drop when coolant subcooling is smaller than ΔT_{fmax}; this, however, happens for $\lambda_* \approx 0.4$.)

Figure 9 shows the temperature difference in the liquid coolant and in the molten drop (see assumptions 4 and 5), for all cases considered, as functions of λ_*. The lowest value of the temperature difference available in the molten drop, i.e. 500 K, is also marked. This figure presents a unique relation between bulk temperatures of the drop and the coolant when it is assumed that the molten drop interface temperature is set at 3000 K (for these temperatures it also determines the value of λ_*). If for a given value of liquid subcooling, ΔT_l, the temperature difference in the drop, ΔT_f, is smaller than that shown in Fig. 9 (for the same value of λ_*), the surface temperature will drop below 3000 K and solidification will occur. The same will happen if for a given temperature difference in the drop, ΔT_f, liquid subcooling is greater than that shown in Fig. 9. It is also worth noting that the above conclusions are valid when one applies this unique relation to the initial temperatures of molten fuel and coolant, i.e. before the former enters the latter (since, in particular, the drop bulk temperature cannot be higher than the initial one). The particle diameter has to be specified.

4.2. *Conclusions*

From Fig. 9 it is clear that for cases UO_2–H_2O (150 bar) and, particularly, for UO_2–Na (when the sodium subcooling is not very small), substantial temperature differences are required to maintain the drop in a molten state. Without such differences the drop–vapour interface temperature will fall below the value assumed (3000 K) at which solidification of the drop will start. A considerably stronger pressure pulse, in the further stages of vapour explosion, is required to induce drop fragmentation if any solidification has occurred.

Although this solidification process is outside the scope of the presented model, three important conclusions, related not only to the coarse pre-mixing stage of vapour explosion, but to the entire phenomenon, can be drawn. These conclusions are based on estimates of the required temperature difference in the molten drop for each of the three cases. Although the model is limited to the stagnation point region, it clearly shows that:

1. When the maximum temperature difference available in the molten drop is lowest (i.e. $\Delta T_{fmax} = 500$ K), the whole drop can be maintained in the molten state, for any liquid subcooling, only in the UO_2–H_2O (1 bar) case.
2. Thermal conditions leading to a large coarse-mixture volume (which can result in an efficient, large-scale vapour explosion) are less restrictive for the UO_2–H_2O (1 bar) case than for the other cases (UO_2–Na being the most difficult to sustain if the sodium subcooling is not very small).
3. Comparison of the two UO_2–H_2O cases shows that increasing the system pressure reduces the conditions necessary to sustain a fuel drop in the molten state. Therefore, the possibility of a steam explosion reduces with the system's pressure.

The last two conclusions, which are based on the model presented, are supported by the experimental evidence and other theoretical works related to the vapour explosion subject [1–4, 9, 10].

REFERENCES

1. M. Corradini, K. Y. Bang and J. Tang, Fuel–coolant interactions and vapour explosions, *Proc. U.S. Nuclear Regulatory Commission*, NUREG/CP-0105, Vol. 2, pp. 223–247 (1989).
2. U. S. Nuclear Regulatory Commission, Severe Accident Risks, Summary Report, NUREG 1150, Second Draft for Peer Review (1989).
3. T. G. Theofanus *et al.*, An assessment of steam-explosion-induced containment failure, *Nucl. Sci. Engng* **97**, 259–326 (1987).
4. T. R. Fodemski, A study on thermal explosion as applied to molten fuel–coolant interaction, *Archiwm Termodynamiki* **4**, 257–295 (1986).
5. V. K. Dhir and G. D. Purohit, Subcooled film boiling heat transfer from spheres, *Nucl. Engng Des.* **47**, 49–66 (1978).
6. M. Epstein and G. M. Hauser, Subcooled forced-convection film boiling in the forward stagnation region of a sphere or cylinder, *Int. J. Heat Mass Transfer* **23**, 179–189 (1980).
7. T. R. Fodemski, The influence of liquid viscosity and system pressure on stagnation point vapour thickness during forced convection–film boiling, *Int. J. Heat Mass Transfer* **28**, 69–80 (1985).
8. Y. Zvirin, G. F. Hewitt and D. B. R. Kenning, Experimental study of drag and heat transfer during boiling on free-falling spheres, *Proc. 7th Natn. Conf U.I.T.*, Florence, Italy, pp. 151–162 (1989).
9. A. Inoue and S. G. Bankoff, Destabilization of film boiling due to arrival of a pressure shock, *Trans. ASME J. Heat Transfer* **103**, 459–464 (1981).
10. M. L. Corradini, Modelling film boiling destabilization due to a pressure shock arrival, *Nucl. Sci. Engng* **84**, 196–205 (1983).
11. T. R. Fodemski, Experimental investigation of steady and destabilized forced convection–film boiling on a hemisphere using the electrical capacity method, *Proc.*

8th Int. Heat Transfer Conf., San Francisco, U.S.A., Vol. 5, pp. 2142–2148 (1986).
12. J. B. Knowles, A mathematical model of vapour film destabilisation, AEEW-R 1933, AEE WINFRITH (1985).
13. W. J. Prosnak, On viscous flow near the stagnation point on an interface, AFOSR 1952, Princeton Univ. Dept. Aero. Engng, Rep. 563 (1961).
14. B. T. Chao, Transient heat and mass transfer to a translating droplet, *J. Heat Transfer, Trans. ASME* 273–280 (1969).
15. B. T. Chao, Motion of spherical bubble in a viscous liquid at large Reynolds number, *Physics Fluids* **5**, 69–79 (1962).
16. T. A. Dullforce, The spontaneous triggering of small-scale vapour explosion, Ph.D. Thesis, Univ. of Aston, Birmingham (1981).
17. Y. Iida, T. Takashima and R. Akiyoshi, A study of the vapour explosion mechanism with single drops of high temperature liquids and volatile liquids, *Trans. JSME* **1777**, 452–476 (1986).
18. D. L. Hagrman and G. A. Reymann, *A Handbook of Material Properties for Use in the Analysis of Light Water Reactor Fuel Rod Behaviour*, U.S. Nuclear Regulatory Commission, NUREG/CR-0497 (1979).
19. E. Schmidte, *Properties of Water and Steam in SI Units*, Third Enlarged Printing. Springer, Berlin (1982).
20. N. B. Vargaftik, *Tables on the Thermophysical Properties of Liquids and Gases in Normal and Dissociated States*, 2nd Edn. Halsted Press, New York (1975).
21. O. J. Foust, *Sodium–NaK Engineering Handbook*, Vol. 1. Gordon & Breach, New York (1972).
22. J. K. Fink, Argonne Natn. Lab. Rept. ANL-CEN-RSD-82-4 (1982).

APPENDIX

Equation (1), neglecting the inertia effect, simplifies to

$$F_v'''(\eta_v) = -1. \tag{A1}$$

Since $F_v(0) = 0$, its solution can be written in the form:

$$F_v(\eta_v) = -\tfrac{1}{6}\eta_v^3 + \tfrac{1}{2}C_1\eta_v^2 + C_2\eta_v. \tag{A2}$$

From boundary and matching conditions on interface II (equations (6) and (17)), we have

$$C_2 = \alpha_1 F_f'(0), \quad C_1 = -\alpha_2 F_f''(0)$$

and

$$C_1 = -\alpha_2 a_1\left(1-\frac{C_2}{\alpha_1}\right)\sqrt{\left(1+b_1\frac{C_2}{\alpha_1}\right)}. \tag{A3}$$

Using the last equation, the solution of equation (A1) can be written in the form

$$F_v(\eta_v) = -\tfrac{1}{6}\eta_v^3 - \tfrac{1}{2}\alpha_2 a_1\left(1-\frac{C_2}{\alpha_1}\right)\sqrt{\left(1+b_1\frac{C_2}{\alpha_1}\right)}\eta_v^2 + C_2\eta_v \tag{A4}$$

and

$$F_v'(\eta_v) = -\tfrac{1}{2}\eta_v^2 - \alpha_2 a_1\left(1-\frac{C_2}{\alpha_1}\right)\sqrt{\left(1+b_1\frac{C_2}{\alpha_1}\right)}\eta_v + C_2 \tag{A5}$$

$$F_v''(\eta_v) = -\eta_v - \alpha_2 a_1\left(1-\frac{C_2}{\alpha_1}\right)\sqrt{\left(1+b_1\frac{C_2}{\alpha_1}\right)}. \tag{A6}$$

Equations (A4)–(A6) can now be used in boundary and matching conditions on interface I (equations (6) and (16)); therefore we have:

$$F_l(0) = \frac{1}{\beta_2}F_v(\eta_v^\delta)$$

$$F_l'(0) = \frac{1}{\beta_1}F_v'(\eta_v^\delta)$$

$$F_l''(0) = \frac{1}{\beta_1\beta_2}F_v''(\eta_v^\delta)$$

and

$$F_v''(\eta_v^\delta) = \beta_1\beta_2\left\{a_1 + \frac{a_2}{\beta_2}F_v(\eta_v^\delta) + a_3\left[\frac{1}{\beta_2}F_v(\eta_v^\delta)\right]^2\right\} \times \sqrt{\left(1+\frac{b_1}{\beta_1}F_v'(\eta_v^\delta)\left\{1+\frac{b_2}{\beta_2}F_v(\eta_v^\delta)+b_3\left[\frac{1}{\beta_2}F_v(\eta_v^\delta)\right]^2\right\}\right)}. \tag{A7}$$

It is clear from the last equation that for given value of η_v^δ (i.e. for assumed velocity gradient A_v and vapour thickness δ) one can find the C_2 constant and the velocity field in the vapour gap is therefore determined. Further, using relation (A4) in equations (10)–(13), (22) and (23) the temperature field and heat fluxes, on both interfaces, are determined. These heat fluxes can be expressed by the heat flux for simple conduction through stagnant vapour of the same thickness δ (see equation (24)) in the following way:

$$q_\delta = -k_v\left.\frac{dT_v}{dy}\right|_{y=\delta} = k_v t_v'(\eta_v^\delta)\frac{d\eta_v}{dy}(T_w - T_s) = q_0\frac{\eta_v^\delta e_v(\eta_v^\delta)}{E_v(\eta_v^\delta)} \tag{A8}$$

$$q_w = -k_v\left.\frac{dT_v}{dy}\right|_{y=0} = k_v t_v'(0)\frac{d\eta_v}{dy}(T_w - T_s) = q_\delta\frac{1}{e_v(\eta_v^\delta)} \tag{A9}$$

where

$$e_v(\eta_v) = \exp\left[-2Pr\int_0^{\eta_v} F_v(\xi)\,d\xi\right]$$

$$E_v(\eta_v) = \int_0^{\eta_v} e_v(\xi)\,d\xi.$$

From equations (A8) and (A9) it is clear that coefficients d_3 and d_4, appearing in equation (25), are

$$d_3 = \frac{1}{e_v(\eta_v^\delta)} \quad \text{and} \quad d_4 = \eta_v^\delta\frac{e_v(\eta_v^\delta)}{E_v(\eta_v^\delta)}.$$

Note that once the temperature difference across the vapour gap $(T_w - T_s)$ is known, one can conduct the calculation for all three phases in a simple manner.

For example, assuming velocity gradient A_v and vapour thickness δ (or η_v^δ or λ_*), coefficients d_{1l}, d_{2l} (for liquid coolant) and d_{2f} (for molten drop; note that $d_{1f} \equiv 1$, since there is no evaporation on interface II) can be determined. Although all these coefficients are related to $F_l(0)$ (see Figs. 2 and 3) they are in fact, through the first matching condition on interface I (i.e. $F_v(\eta_v^\delta) = \beta_2 F_l(0)$), also dependent on η_v^δ (or δ or λ_*). As mentioned in Section 2.2, coefficients d_{1l}, d_{2l} and d_{2f} are the measures of effects: (i) evaporation (from the interface) and (ii) viscous forces (acting in the interface vicinity), on the degree of departure of the interface heat fluxes (q_l and q_f) from the frictionless case (as expressed by equation (14)). Summarizing: for given values of T_w, T_s and η_v^δ (δ or λ_*) one can determine temperature differences both in the molten drop $(T_{f\infty} - T_w)$ and in the liquid coolant $(T_s - T_{l\infty})$, using heat balances on interfaces (see equation (25)).

EBULLITION EN FILM AVEC CONVECTION FORCEE DANS LA REGION D'ARRET D'UNE GOUTTE FONDUE ET APPLICATION AUX EXPLOSIONS DE VAPEURS

Résumé—On explore le mécanisme de transfert de chaleur lié à l'explosion thermique. Le modèle théorique de l'ébullition en film avec convection forcée est présenté pour la région d'arrêt d'une goutte fondue asymétrique ; il prend en compte le fait que la substance chaude est fondue. Les équations d'impulsion au point d'arrêt (Falkner–Skan) et d'énergie, pour les liquides froids ou chauds et pour la couche de vapeur, sont résolues numériquement avec un large domaine de conditions aux interfaces. Le modèle présenté, en couvrant un large domaine de conditions et de paramètres, est plus général que les cas discutés dans d'autres publications. Pour cette raison les résultats peuvent être appliqués non seulement à l'étape du prémélange grossier à l'explosion de vapeur mais aussi à d'autres situations où la convection forcée avec trois phases apparaît sur un corps axisymétrique.

FILMSIEDEN BEI ZWANGSKONVEKTION IM STAUGEBIET EINES GESCHMOLZENEN TROPFENS UND DIE ANWENDUNG AUF DAMPFEXPLOSIONEN

Zusammenfassung—Die vorliegende Arbeit wurde im Rahmen einer Untersuchung der Wärmeübergangsmechanismen bei thermischen Explosionen durchgeführt. Das theoretische Modell des Filmsiedens bei Zwangskonvektion in der Nähe des Staupunktes eines achsensymmetrischen geschmolzenen Tropfens wird vorgestellt. Das Modell ist besonders für die Vormischungsstufe der Dampfexplosion von Bedeutung. Es berücksichtigt die Tatsache, daß die heiße Substanz in dieser Stufe geschmolzen ist. Die Impulsgleichung (nach Falkner/Skan) und die Energieerhaltungsgleichung am Staupunkt werden für kalte und heiße Flüssigkeiten sowie für die Dampfschicht numerisch gelöst, und zwar für einen weiten Bereich der Randbedingungen an der Oberfläche. Das vorgestellte Modell, das einen weiten Bereich von Bedingungen und Parametern abdeckt, ist viel allgemeingültiger als die in anderen Veröffentlichungen behandelten Fälle. Aus diesem Grund können die Ergebnisse nicht nur auf die Vormischstufe der Dampfexplosion angewandt werden, sondern auch auf andere Fälle, bei denen eine dreiphasige Zwangskonvektion an einem achsensymmetrischen Körper auftritt.

ПЛЕНОЧНОЕ КИПЕНИЕ ПРИ ВЫНУЖДЕННОЙ КОНВЕКЦИИ В ЗАСТОЙНОЙ ЗОНЕ РАСПЛАВЛЕННОЙ КАПЛИ И ЕГО ИСПОЛЬЗОВАНИЕ В СЛУЧАЯХ ВЗРЫВА ПАРА

Аннотация—Исследуется механизм теплопереноса при тепловом взрыве. Преложена теоретическая модель пленочного кипения при вынужденной конвекции в застойной зоне осесимметричной расплавленной капли. Модель опмсывает стадию предварительного смешивания при взрыве пара, когда горячее вещество расплавлено. Численно решаются уравнения сохранения импульса (Фолкнера–Скэна) и энергии для ненагретых и нагретых жидкостей и для слоя пара при самых различных граничных условиях на границах раздела. Предложенная модель для широкого диапазона условий и параметров является более обобщенной, чем обсуждаемые в других публикациях. По этой причине полученные результаты могут применяться не только для стадии предварительного смешивания при взрыве пара, но и в других случаях, когда трефазная вынужденная конвекция происходит на осесимметричном теле.